

Localization and mutagenesis of the sorting signal binding site on sortase A from *Staphylococcus aureus*

Chu Kong Liew^{a,b}, Brenton T. Smith^a, Rosemarie Pilpa^{a,b}, Nuttee Suree^{a,b}, Udayar Ilangovan^{a,b}, Kevin M. Connolly^{a,b}, Michael E. Jung^{a,1}, Robert T. Clubb^{a,b,c,*}

^aDepartment of Chemistry and Biochemistry, University of California, Los Angeles, 405 Hilgard Avenue, Los Angeles, CA 90095-1570, USA

^bUCLA-DOE Institute for Genomics and Proteomics, University of California, Los Angeles, 405 Hilgard Avenue, Los Angeles, CA 90095-1570, USA

^cMolecular Biology Institute, University of California, Los Angeles, 405 Hilgard Avenue, Los Angeles, CA 90095-1570, USA

Received 4 May 2004; revised 21 June 2004; accepted 29 June 2004

Available online 6 July 2004

Edited by Pascale Cossart

Abstract Surface proteins in Gram-positive bacteria are anchored to the cell wall by the action of sortase enzymes. The *Staphylococcus aureus* sortase A (SrtA) protein anchors proteins by recognizing a cell wall sorting signal containing the amino acid sequence LPXTG. To understand how SrtA binds this sequence, we carried out NMR studies of new peptidyl-cyanoalkene and peptidyl-sulfhydryl inhibitors that contain the sorting signal sequence LPAT. These studies combined with amino acid mutagenesis identified a catalytically important and conserved binding surface formed by residues A118, T180, and I182. Compatible with its recently proposed role as a general base, R197 is also shown to be required for catalysis. © 2004 Published by Elsevier B.V. on behalf of the Federation of European Biochemical Societies.

Keywords: Sortase; Cell wall; Inhibitor; NMR

1. Introduction

Gram-positive bacteria infect humans through an array of surface associated proteins that promote bacterial adhesion to specific organ tissues, resistance to phagocytic killing, as well as host cell invasion. Many surface proteins are covalently anchored to the bacterial cell wall by the action of sortase enzymes, a family of novel transpeptidases (reviewed in [1–5]). The sortase A (SrtA) protein from *Staphylococcus aureus* is the most extensively characterized sortase enzyme [6] and anchors surface proteins that contain a C-terminal sorting signal consisting of a conserved LPXTG motif (where X is any amino acid), a hydrophobic domain and a tail of mostly positively

charged residues [7,8]. During cell wall anchoring, SrtA cleaves surface proteins in between the threonine and the glycine of the LPXTG motif [9]. The carboxyl-group of threonine is then amide linked to the amine-group of the cell wall precursor lipid II [undecaprenyl-pyrophosphate-MurNac(-L-Ala-D-iGln-L-Lys(NH₂-Gly₅)-D-Ala-D-Ala)-β-1-4-GlcNac] [10,11], which is subsequently incorporated into the peptidoglycan via the transglycosylation and transpeptidation reactions of bacterial cell wall synthesis [12]. SrtA and related proteins may be excellent targets for new broad-spectrum anti-infective agents, since sortase-like enzymes and the LPXTG signal are universally conserved in Gram-positive bacteria [5,13,14], and sortase (–) strains of *S. aureus* [15–17], *Listeria monocytogenes* [18,19] and *Streptococcus gordonii* [20] display defects in their virulence.

The *S. aureus* SrtA protein adopts a novel fold with an active site that contains two catalytically essential side chains, H120 and C184 [21]. The sulfhydryl group of C184 nucleophilically attacks the carbonyl carbon at the scissile T–G peptide bond (in the LPXTG motif) to form a thio-acyl bond with the substrate. Several lines of evidence support a central role for C184 in catalysis: (i) it is completely conserved in sortase enzymes [5], (ii) it is essential for catalysis, (iii) methyl methanethiosulfonate, a compound that preferentially reacts with thiolate ions abolishes sortase activity [22] and (iv) mass spectrometry reveals a reaction intermediate with a mass consistent with a thio-acyl enzyme–substrate complex [23]. H120 also plays an important role in catalysis: like C184, it is completely conserved and its mutation to alanine eliminates enzyme activity [24]. Lastly, R233 in the structurally related *S. aureus* sortase B (SrtB) enzyme has also been suggested to participate in catalysis [25] although the catalytic importance of this amino acid in SrtB or the equivalent residue in SrtA (R197) is yet to be confirmed experimentally.

Although residues H120 and C184 in SrtA form the active site, the surface on the enzyme used to recognize the LPXTG sorting signal is still not known, since all the structures of this enzyme class that have been solved to date lack their sorting signal substrates. Here, we describe the synthesis and inhibitory properties of a novel mechanism-based cyanoalkene inhibitor that contains the amino acid sequence of the SrtA substrate (LPAT). NMR studies of SrtA-cyanoalkene and SrtA-sulfhydryl inhibitor complexes and targeted mutagenesis

* Corresponding author. Fax: +1-310-206-4749.

E-mail addresses: jung@chem.ucla.edu (M.E. Jung), rclubb@mbi.ucla.edu (R.T. Clubb).

¹ Fax: +1-310-206-3722.

Abbreviations: SrtA, sortase A; SrtB, sortase B; EDCI, 1-[3-(dimethylamino)propyl]-3-ethylcarbodiimide hydrochloride; Cbz, benzyloxycarbonyl; DMAP, 4-(dimethylamino)pyridine; TBDPS, *t*-butyldiphenylsilyl; DIBAL-H, diisobutylaluminum hydride; TFA, trifluoroacetic acid; DTT, dithiothreitol; HPLC, high performance liquid chromatography; HSQC, heteronuclear single quantum correlation; DMSO, dimethyl sulfoxide

reveal a hydrophobic surface on strands $\beta 4$ and $\beta 7$ that binds the sorting signal. Many residues within the surface are essential for catalysis and are conserved in other sortases that anchor proteins bearing the LPXTG motif.

2. Materials and methods

2.1. Reagents

Residues 60–206 of wild-type sortase A (SrtA_{AN59}), and a single amino acid mutant of the protein containing a cysteine to alanine substitution at position 184 (C^{184A}SrtA_{AN59}), were overexpressed from plasmids pSRTA and pHTT45, respectively [21,24]. The expression, uniform isotopic labeling (where applicable), and purification have been previously described [21]. The fluorescent peptide substrate d-QALPETGEE-e (where d is Dabcyl (4-[[4-(dimethylamino)phenyl]-azo]-benzoyl-) and e is EDANS ([[2-aminoethyl]-amino]naphthlene-1-sulfonyl-)) was purchased from Synpep (Dublin, CA).

2.2. Site directed mutagenesis of SrtA

Single amino acid mutations of SrtA were produced using the Quikchange site-directed mutagenesis kit (Stratagene, La Jolla, CA) with pSRTA as the template. The identity of the SrtA mutants (A118E, T180K, I182S and R197E) was confirmed by DNA sequencing.

2.3. Synthesis of the cyanoalkene inhibitor

The cyanoalkene inhibitor (Fig. 1A, 1) was synthesized using solution phase methodology (Fig. 1A). The leucine–proline–alanine portion of the synthesis was carried out using standard amino acid coupling reactions (EDCI, 1-[3-(dimethylamino)propyl]-3-ethylcarbodiimide hydrochloride; DMAP, 4-(dimethylamino)pyridine) starting with the protected amino acid Cbz–Leucine–OH. L-Threonine was fully protected as the *N*-Boc-threonine methyl ester with the alcohol protected as the TBDPS (*t*-butyldiphenylsilyl) silyl ether (Fig. 1A, 2) in three steps. The ester was then reduced to the aldehyde using DIBAL-H (diisobutylaluminum hydride) which was immediately reacted without purification with diethyl (cyanomethyl)phosphonate (Fig. 1A, 3) to give the desired cyanoalkene functionality (Fig. 1A, 4) in good yields. Removal of the Boc group with TFA followed by coupling the amine with the Cbz-protected tripeptide gave the desired tetrapeptide. Removal of the TBDPS group with HF in acetonitrile gave the cyanoalkene inhibitor (Fig. 1A, 1). Purification of the inhibitor was done using silica gel chromatography and its structure was confirmed by ¹H NMR spectroscopy. The details of the production of the peptidyl-sulfhydryl compound and the NMR studies of its complex with SrtA_{AN59} will be reported elsewhere.

2.4. NMR spectroscopy of the SrtA-cyanoalkene complex

A 15-fold molar excess of the cyanoalkene inhibitor (dissolved in dimethyl sulfoxide) was added to ¹⁵N-SrtA_{AN59} (1.3 ml of a 184 μ M solution) in buffer I (pH 8.0, 50 mM Tris–HCl, 100 mM NaCl and 2.5 mM DTT). The mixture was incubated on a rotating wheel at room temperature and the complex was purified using reverse phase HPLC on a C18 column (Waters, Milford, MA). The purified complex was then lyophilized and resuspended in buffer G (pH 6.0, 25 mM Na Acetate, 100 mM NaCl, 0.5 mM DTT and 7% D₂O) for NMR spectroscopy. NMR experiments were carried out at 306 K on a Bruker DRX500 spectrometer equipped with a triple resonance cryoprobe using a sample of purified ¹⁵N-SrtA_{AN59}-inhibitor complex (~130 μ M) in buffer G. A ¹⁵N-¹H HSQC spectrum of the complex was acquired with 2048 complex *t*₂ points and 200 complex *t*₁ points.

2.5. Enzyme assays

Fluorescent measurements of the enzymatic activity of SrtA mutants were performed in 96-well microtiter plates as previously described [26]. Reactions contained 50 μ M of mutant enzyme in buffer R (50 mM Tris–HCl, pH 7.5, 150 mM NaCl, 5 mM glycine and 5 mM CaCl₂). The d-QALPETGEE-e substrate was dissolved in dimethyl sulfoxide and added to the reaction to a final concentration of 25 μ M, for a total reaction volume of 200 μ l. Measurements of SrtA_{AN59} activity in the presence of the cyanoalkene inhibitor were conducted as outlined for the mutant enzymes except that inhibition reactions contained 5 μ M

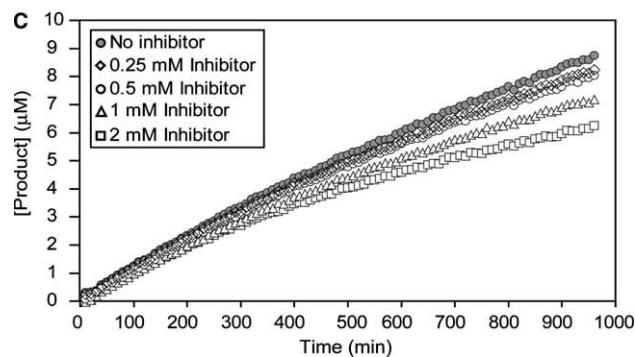
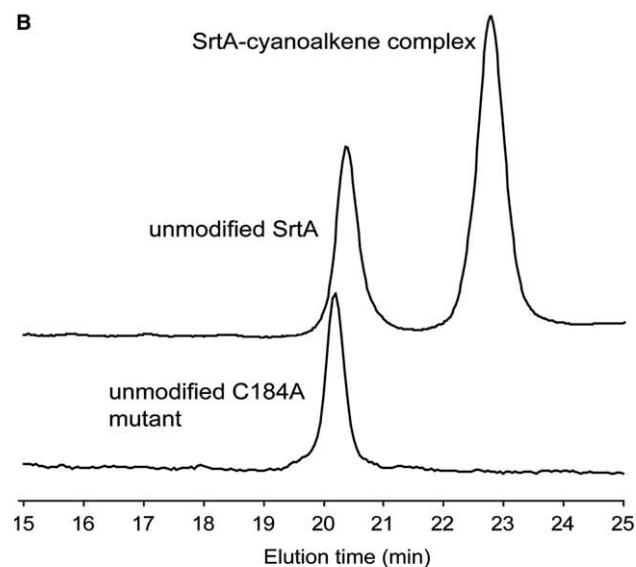
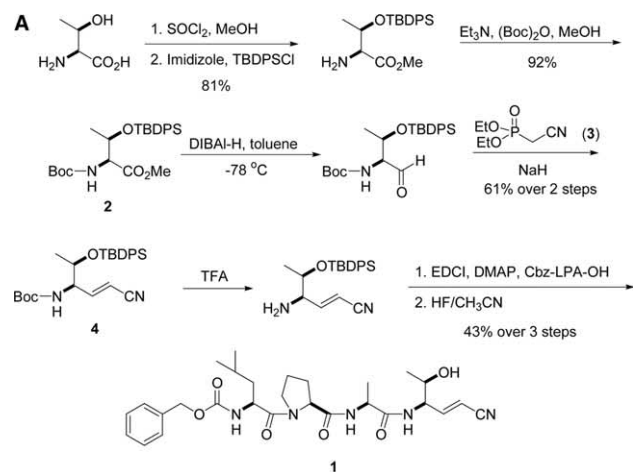


Fig. 1. (A) Strategy for synthesis of the peptide cyanoalkene inhibitor of SrtA. (B) HPLC elution profiles of the inhibitor incubated with SrtA (top) and the C184A mutant of SrtA (bottom). (C) Progress curves of cyanoalkene inhibition of SrtA. K_i and k_i were calculated from the curves as described in [27]. SrtA catalyzed the transpeptidation of the d-QALPETGEE-e substrate with a K_m of 4.1×10^{-5} and a k_{cat} of $7.6 \times 10^{-6} \text{ s}^{-1}$, and are comparable to previously published values [31].

SrtA_{AN59} and cyanoalkene inhibitor (250, 500, 1000 or 2000 μ M) in buffer R. The inhibition parameters K_i and k_i were calculated as previously described [27]. In the transpeptidation assay 15 μ M of sortase was incubated with 10 μ M of d-QALPATGEE-e (buffer: 50 mM Tris–HCl, pH 7.5, 150 mM NaCl, 5 mM glycine, 5 mM CaCl₂, in a 520 μ l

reaction volume). After constant mixing at 37 °C for 16 h, the reaction was stopped by the addition of 500 μ l of 0.1% TFA in water (Buffer A). The products were then separated using reverse phase HPLC on a C18 column (Waters, Milford, MA) using a gradient of 0–50% of buffer B (90% CH₃CN/10% water/0.1% TFA). The products were detected at 475 nm and verified by mass spectrometry.

3. Results and discussion

With the long term goal of developing anti-infective agents that disrupt sortase activity, we synthesized a mechanism based cyanoalkene inhibitor and studied how it interacts with *S. aureus* SrtA. The cyanoalkene inhibitor contains the sorting signal sequence of the SrtA substrate (L–P–A–T–G), but replaces the scissile T–G amide bond with a cyanoalkene group (C=C–CN) (Fig. 1A). Thus, the SrtA-inhibitor interaction allowed us to gain insights into the structural basis of substrate recognition. It was anticipated that SrtA interactions with the

peptide portion of the compound would deliver the cyanoalkene group to the active site, enabling it to irreversibly modify the thiol of C184. Wild-type SrtA was incubated with excess inhibitor and the products were analyzed by reverse phase HPLC (Fig. 1B) and mass spectrometry. Incubation results in the formation of a single new species whose mass is consistent with a single inhibitor molecule covalently bound to SrtA. In contrast, no modification occurs when the inhibitor is incubated with SrtA bearing a C184A mutation, indicating that it specifically modifies the side chain of C184.

The inhibitory properties of the new compound were assessed in vitro by monitoring how it altered the SrtA-catalyzed hydrolysis of an internally quenched fluorescent substrate analogue (d–Q–A–L–P–E–T–G–E–E–e). Typical progress curves of the reaction in the presence of 250, 500, 1000 and 2000 μ M of the inhibitor are shown in Fig. 1C, and are consistent with the compound irreversibly modifying SrtA. From the progress curves at pH 7.5, the K_i of the cyanoalkene inhibitor was

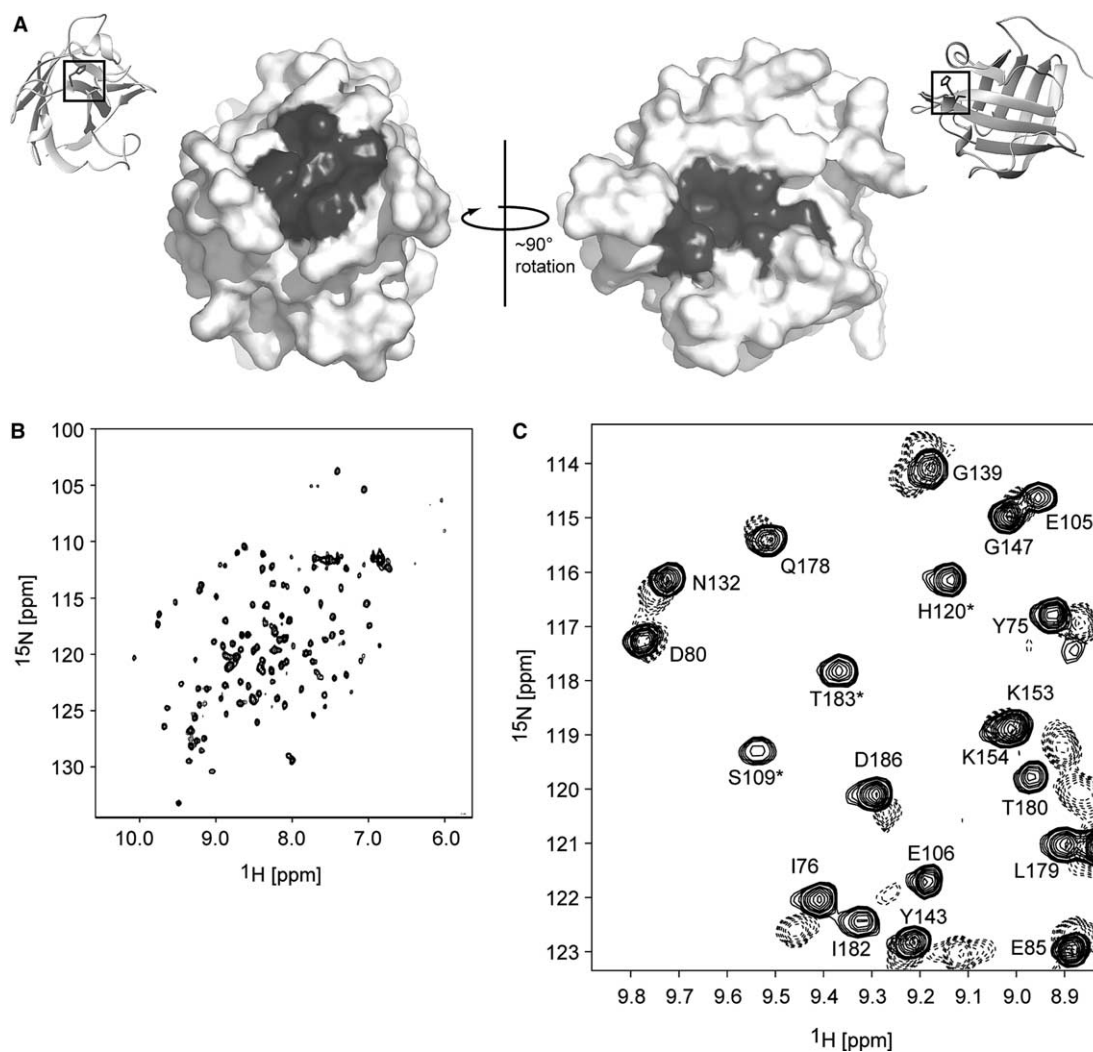


Fig. 2. Location of the inhibitor binding site on SrtA. (A) The two possible binding surfaces for the LPXTG cell wall sorting. Left, the surface formed mainly by residues preceding strands β 4 (H120, F122) and β 8 (D185, D186, Y187), and residues in helix 1 (P94, N98). Right, the surface formed mainly by residues in strands β 4 (A118), β 7 (I182, C184) and the β 3– β 4 (A104, E105), β 6– β 7 (L169, E171) and β 7– β 8 (V193, W194, R197) loops. For reference, a ribbon representation in the same orientation is shown next to each surface plot. The side chains of the catalytic residues, C184 and H120, are shown and boxed. (B) ^1H – ^{15}N HSQC spectrum of the SrtA_{AN59}–cyanoalkene complex. (C) Overlay of a selected portion of the ^1H – ^{15}N HSQC spectrum of SrtA_{AN59} and the SrtA_{AN59}–cyanoalkene complex. Peaks from the free protein spectrum are represented with continuous lines while dashed lines represent peaks from the spectrum of the complex. Residues with an asterisk are significantly perturbed upon inhibitor binding.

calculated to be 1.0×10^{-4} M and the first-order rate constant of inactivation (k_i) is $6.3 \times 10^{-4} \text{ min}^{-1}$. The K_i is comparable to the measured K_m of SrtA for the fluorogenic substrate (4.1×10^{-5} M), consistent with their similar structures. Both natural [28] and synthetic [26,27] SrtA inhibitors have been described. In addition to the cyanoalkene moiety described in this study, inhibitors that pair thiol modifying vinyl sulfone ($\text{C}=\text{C}-\text{SO}_2\text{Ph}$; $k_i = 4 \times 10^{-4} \text{ min}^{-1}$) [27], diazomethane ($-\text{CH}=\text{N}_2$; $k_i = 5.8 \times 10^{-3} \text{ min}^{-1}$), and chloromethane ($-\text{CH}_2\text{Cl}$; $k_i = 1.2 \times 10^{-2} \text{ min}^{-1}$) [26] groups to the sorting signal peptide have been used. The *in vitro* k_i of the cyanoalkene compound indicates that it has intermediate reactivity, but the true utility of these different chemical approaches awaits *in vivo* studies. The peptide portion of the cyanoalkene inhibitor is required for inhibition, since compounds in which the leucine is deleted do not inhibit the enzyme (unpublished results).

As the cyanoalkene inhibitor contained the sorting signal (LPAT) recognized by SrtA, it could be used to localize the substrate-binding site on the protein. Inspection of the SrtA solution structure reveals two potential binding sites that are positioned on opposite sides of the active site (Fig. 2A). To distinguish between these sites, we used NMR spectroscopy to study how SrtA interacts with the cyanoalkene inhibitor. The ^1H - ^{15}N HSQC spectrum of the purified SrtA_{ΔN59}-cyanoalkene complex is displayed in Fig. 2B, revealing that the modified protein remains folded, as judged by the existence of a set of well resolved ^1H - ^{15}N cross-peaks. Unfortunately, the chemical shifts of the complex could not be assigned because limiting amounts of inhibitor and the slow rate of modification prevented the production of large quantities of the complex (the concentration of the SrtA_{ΔN59}-cyanoalkene complex was $\sim 130 \mu\text{M}$). However, the general effects of inhibitor binding could be deduced by comparing the ^1H - ^{15}N HSQC spectrum of the complex with the corresponding spectrum of the unmodified SrtA_{ΔN59} protein for which complete resonance assignments are known [29]. An overlay of the two spectra reveals that the majority of backbone amide groups exhibit

similar ^1H - ^{15}N chemical shifts (Fig. 2C). However, several ^1H - ^{15}N correlations in the spectra of the SrtA_{ΔN59}-cyanoalkene complex are either severely broadened or are at sufficiently distinct chemical shifts as to prevent their assignment by comparison to the spectra of the unmodified SrtA_{ΔN59} protein (for example S109, H120 and T183 in Fig. 2C). Mapping those residues that exhibit the largest chemical shift changes onto the structure of SrtA enables the localization of the inhibitor-binding site, since it is expected that the magnetic environment of the residues that form the binding site will be significantly

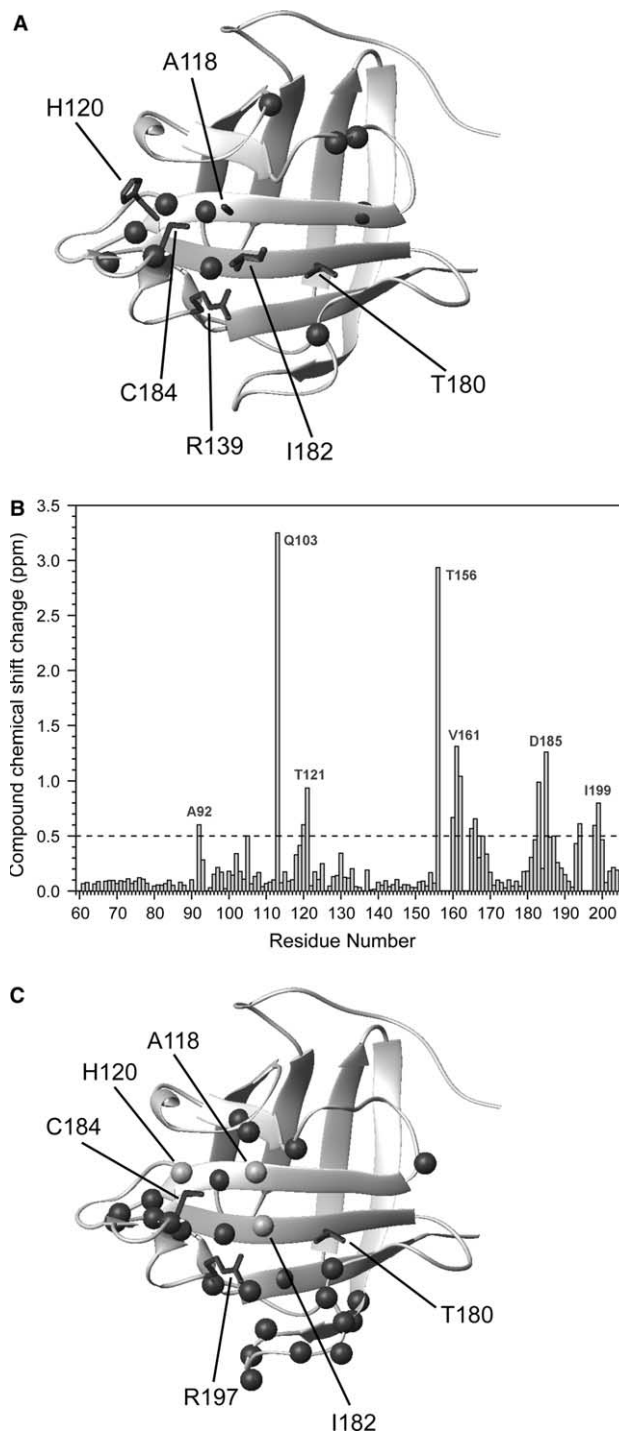


Fig. 3. Chemical shift perturbation of SrtA resonances upon inhibitor complex formation. Chemical shift changes ($\Delta\delta$) of the backbone ^{15}N and ^1H resonances for residues in the SrtA complexes compared to free SrtA were calculated according to $\Delta\delta = [(\delta_{\text{HN}})^2 + (\delta_{\text{N}}/6.49)^2]^{1/2}$ from [32]. (A) Ribbon representation of SrtA depicting the residues that are significantly perturbed upon modification by the peptidyl-cyanoalkene inhibitor. The chemical shift change for a particular residue was calculated by comparing its peak in the free protein spectrum to the closest peak (in terms of ^1H and ^{15}N chemical shift) in the spectrum of the complex. Hence, it is important to note that a residue whose peak shifts significantly upon inhibitor binding may not necessarily be depicted in this figure if there are peaks in the spectrum of the complex that are close to its original position in the free protein spectrum. (B) Chemical shift changes ($\Delta\delta$) in the SrtA-sulfhydryl complex compared to free SrtA. The dotted line at 0.3 ppm indicates the level of significance. (C) Ribbon representation of SrtA depicting the residues that are significantly perturbed when the enzyme is modified with the peptidyl-sulfhydryl inhibitor. Almost complete (97%) assignments were obtained for the spectrum of the SrtA-sulfhydryl complex. In figures (A) and (C), residues whose amide resonances undergo large chemical shift changes ($\Delta\delta > 0.2$ in A and $\Delta\delta > 0.3$ in B) are depicted as spheres. The sidechains of the catalytic residues, C184 and H120 as well as the residues that were mutated (A118, T180, I182 and R197) are shown in (A). The same residues are shown in (C) except that the sidechains of H120, A118 and I182 are replaced by grey spheres to indicate that their amide resonances exhibited significant ($\Delta\delta > 0.3$) chemical shift perturbation upon peptidyl-sulfhydryl inhibitor binding.

altered upon contact with the inhibitor. Fig. 3A shows that the most significantly perturbed residues cluster mainly to two regions: (i) residues immediately proximal to the catalytic H120 and C184, and (ii) residues located within and around the loop connecting strands $\beta 3$ and $\beta 4$. It is important to note that the ^1H - ^{15}N resonances of residues in strands $\beta 4$ and $\beta 7$ are located in a crowded region of the HSQC spectrum, making it difficult to deduce the effects of inhibitor binding simply by spectral comparison. The NMR data are therefore most compatible with the covalently bound inhibitor positioned such that its threonine is proximal to C184 and its leucine-proline-alanine portion is in contact with residues in strands $\beta 4$ and $\beta 7$, and the loops that surround this site (the $\beta 3$ - $\beta 4$ and $\beta 6$ - $\beta 7$ loops).

To further define the binding surface, a peptidyl-sulphydryl compound was used to modify $\text{SrtA}_{\Delta\text{N}59}$ and this complex was studied by NMR. This compound also contains the amino acid sequence LPAT, but replaces the terminal carboxyl group with $-\text{CH}_2\text{-SH}$. Upon incubation with $\text{SrtA}_{\Delta\text{N}59}$ it forms a disulfide bond to the thiol of C184 and thus mimics the thio-acyl intermediate. The NMR spectra of the $\text{SrtA}_{\Delta\text{N}59}$ -sulphydryl complex are well dispersed, enabling the assignment of 97% of the ^1H , ^{13}C and ^{15}N chemical shifts of the backbone atoms of $\text{SrtA}_{\Delta\text{N}59}$ in the complex, using conventional triple resonance techniques (data not shown). Fig. 3B displays a histogram plot of the ^{15}N and ^1H chemical shifts of each residue in the $\text{SrtA}_{\Delta\text{N}59}$ -sulphydryl complex compared to free $\text{SrtA}_{\Delta\text{N}59}$. This data shows that peptide binding causes large and localized chemical shift changes in $\text{SrtA}_{\Delta\text{N}59}$. Mapping these changes onto the structure reveals an extensive binding surface involving residues positioned immediately adjacent to C184 in strands $\beta 3$, $\beta 4$ and $\beta 8$, as well as residues within the $\beta 6$ - $\beta 7$ loop (Fig. 3C). The interaction surface for the sulphydryl compound is essentially the same as seen for the cyanoalkene compound (Fig. 3A and C), but it is more extensive because near complete backbone assignments were obtained for the $\text{SrtA}_{\Delta\text{N}59}$ -sulphydryl complex.

Reasoning that surface exposed residues highlighted by the NMR data would contact the sorting signal, we tested the enzymatic importance of residues within and around the interaction surface. Four single amino acid mutations were introduced into residues within strands $\beta 4$ (A118E), $\beta 7$ (T180K, I182S) and $\beta 8$ (R197E) (Fig. 3A). All of the mutant proteins remain folded (as judged by NMR spectroscopy), however the A118E, I182S and R197E mutants are completely inactive, as judged by two different assays, namely, the *in vitro* hydrolysis assay (Fig. 4A) and an HPLC assay that measures transpeptidation (Fig. 4B). Since the surface exposed hydrophobic side chains of A118 and I182 are positioned directly adjacent to C184, it appears likely that they are involved in sorting signal binding. How R197 participates in catalysis is less clear, but the lack of activity observed for the R197E mutant is compatible with this residue functioning to deprotonate the incoming nucleophile (water in this assay), as proposed in a model based on recent crystallographic work [25]. It is tempting to speculate that the least disruptive T180K mutation is due to this residue being positioned at the edge of the signal-binding site.

The localization of the sorting signal binding site on SrtA provides insights into the specificities of other sortase enzymes. A comparison of *S. aureus* SrtA protein with sortase homologs (from *S. suis*, *L. monocytogenes* and *S. pyogenes*) that process the same sorting signal reveals that nearly all of the critical

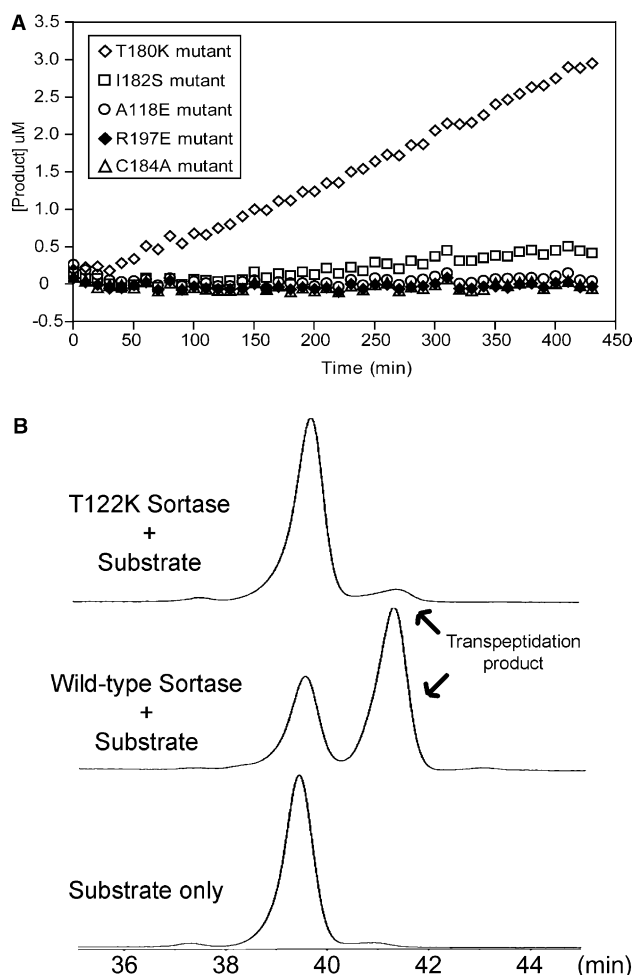


Fig. 4. Characterization of the SrtA mutants. (A) Progress curves of d-QALPATGEE-e hydrolysis by SrtA mutants. Reaction mixtures contained $50 \mu\text{M}$ of each enzyme and $25 \mu\text{M}$ d-QALPATGEE-e in $200 \mu\text{l}$ of buffer R. (B) Transpeptidation assay. In the absence of enzyme only the free d-QALPATGEE-e peptide is observed (bottom trace), but upon incubation with wild-type SrtA the transpeptidation product is produced, d-QALPATG (middle trace). The A118E, I182S, and R197E mutant proteins are completely inactive (data not shown), and the T180K mutant shows only modest activity as compared to the wild type protein (top trace).

amino acid side chains identified in this study are conserved in sortases known to process LPXTG; A118 and T180 are completely conserved, and I182 is semi-conserved. Interestingly, at least two of the catalytically important residues identified in this study are not conserved in SrtB (which processes the sequence NPQTN), suggesting that they contribute to substrate binding specificity (A118 and I182 in SrtA are Y128 and S221 in SrtB , respectively).

Following the submission of this paper, the LPETG binding site on a C184A mutant of $\text{SrtA}_{\Delta\text{N}59}$ ($^{\text{C}184\text{A}}\text{SrtA}_{\Delta\text{N}59}$) was determined by crystallography. In the crystal structure, the threonine at the C-terminal end of the peptide rests near C184 and the N-terminal end contacts strand $\beta 7$ and residues within the $\beta 6/\beta 7$ loop [30]. These results are compatible with our NMR data, which has revealed that the primary interaction surface in solution is the $\beta 6/\beta 7$ loop and the underlying β -sheet (Fig. 3C). A detailed analysis of the structure is not possible, since the coordinates are on hold for one year.

However, the crystal structure suggests that the A118E and I182S mutants are inactive because they disrupt contacts to the threonine in the sorting signal, while the T180K mutant may be defective in binding to the leucine and proline residues in the signal. The role of R197 is unclear, but the R197E mutation may inactivate sortase because it eliminates stabilizing contacts to oxyanion intermediates and/or guanidino mediated proton transfer events required for catalysis. Sortase may recognize the sorting signal through an induced fit mechanism involving changes in the conformational dynamics of the protein, since the three sortase molecules present in the asymmetric unit of the crystal differ in the conformation of the $\beta 6/\beta 7$ loop and this region is disordered in the NMR structure. Moreover, since only one of the three proteins in the asymmetric unit interacts with the peptide because of crystal packing effects, it will be interesting to see if the mode of binding visualized in the crystal structure predominates in the solution state.

Acknowledgements: We thank Dr. Bernard Fung for the use of his fluorimeter and Dr. Kim Phan for technical assistance. This research was supported by NIH grant AI5221701 to M.E.J. and R.T.C. C.K.L. receives a CJ Martin Fellowship from the National Health and Medical Research Council (NHMRC) of Australia.

References

- [1] Navarre, W.W. and Schneewind, O. (1999) *Microbiol. Mol. Biol. Rev.* 63, 174–229.
- [2] Novick, R.P. (2000) *Trends Microbiol.* 8, 148–151.
- [3] Cossart, P. and Jonquieres, R. (2000) *Proc. Natl. Acad. Sci. USA* 97, 5013–5015.
- [4] Mazmanian, S.K., Ton-That, H. and Schneewind, O. (2001) *Mol. Microbiol.* 40, 1049–1057.
- [5] Pallen, M.J., Lam, A.C., Antonio, M. and Dunbar, K. (2001) *Trends Microbiol.* 9, 97–101.
- [6] Mazmanian, S.K., Liu, G., Hung, T.T. and Schneewind, O. (1999) *Science* 285, 760–763.
- [7] Schneewind, O., Model, P. and Fischetti, V.A. (1992) *Cell* 70, 267–281.
- [8] Schneewind, O., Mihaylovapetkov, D. and Model, P. (1993) *Embo J.* 12, 4803–4811.
- [9] Navarre, W.W. and Schneewind, O. (1994) *Mol. Microbiol.* 14, 115–121.
- [10] Ruzin, A. et al. (2002) *J. Bacteriol.* 184, 2141–2147.
- [11] Perry, A.M., Ton-That, H., Mazmanian, S.K. and Schneewind, O. (2002) *J. Biol. Chem.* 277, 16241–16248.
- [12] Strominger, J.L., Izaki, K., Matsushashi, M. and Tipper, D.J. (1967) *Fed. Proc.* 26, 9–22.
- [13] Janulczyk, R. and Rasmussen, M. (2001) *Infect. Immun.* 69, 4019–4026.
- [14] Comfort, D. and Clubb, R.T. (2004) *Infect. Immunol.* 72, 2710–2722.
- [15] Mazmanian, S.K., Liu, G., Jensen, E.R., Lenoy, E. and Schneewind, O. (2000) *Proc. Natl. Acad. Sci. USA* 97, 5510–5515.
- [16] Mazmanian, S.K., Ton-That, H., Su, K. and Schneewind, O. (2002) *Proc. Natl. Acad. Sci. USA* 99, 2293–2298.
- [17] Jonsson, I.M., Mazmanian, S.K., Schneewind, O., Verdrengh, M., Bremell, T. and Tarkowski, A. (2002) *J. Infect. Diseases* 185, 1417–1424.
- [18] Bierne, H. et al. (2002) *Mol. Microbiol.* 43, 869–881.
- [19] Garandeau, C., Reglier-Poupet, H., Dubail, L., Beretti, J.L., Berche, P. and Charbit, A. (2002) *Infect. Immunity* 70, 1382–1390.
- [20] Bolken, T.C., Franke, C.A., Jones, K.F., Zeller, G.O., Jones, C.H., Dutton, E.K. and Hruby, D.E. (2001) *Infect. Immunity* 69, 75–80.
- [21] Ilangovan, U., Ton-That, H., Iwahara, J., Schneewind, O. and Clubb, R.T. (2001) *Proc. Natl. Acad. Sci. USA* 98, 6056–6061.
- [22] Ton-That, H. and Schneewind, O. (1999) *J. Biol. Chem.* 274, 24316–24320.
- [23] Huang, X., Aulabaugh, A., Ding, W., Kapoor, B., Alksne, L., Tabei, K. and Ellestad, G. (2003) *Biochemistry* 42, 11307–11315.
- [24] Ton-That, H., Mazmanian, S.K., Alksne, L. and Schneewind, O. (2002) *J. Biol. Chem.* 277, 7447–7452.
- [25] Zong, Y., Mazmanian, S.K., Schneewind, O. and Narayana, S.V. (2004) *Structure (Camb.)* 12, 105–112.
- [26] Scott, C.J., McDowell, A., Martin, S.L., Lynas, J.F., Vandebroek, K. and Walker, B. (2002) *Biochem. J.* 366, 953–958.
- [27] Connolly, K.M., Smith, B.T., Pilpa, R., Ilangovan, U., Jung, M.E. and Clubb, R.T. (2003) *J. Biol. Chem.* 278, 34061–34065.
- [28] Kim, S.W., Chang, I.M. and Oh, K.B. (2002) *Biosci. Biotechnol. Biochem.* 66, 2751–2754.
- [29] Ilangovan, U., Iwahara, J., Ton-That, H., Schneewind, O. and Clubb, R.T. (2001) *J. Biomol. NMR* 19, 379–380.
- [30] Zong, Y., Bice, T.W., Ton-That, H., Schneewind, O. and Narayana, S.V. *J. Biol. Chem.* (in press).
- [31] Ton-That, H., Mazmanian, S.K., Faull, K.F. and Schneewind, O. (2000) *J. Biol. Chem.* 275, 9876–9881.
- [32] Ayed, A., Mulder, F.A., Yi, G.S., Lu, Y., Kay, L.E. and Arrowsmith, C.H. (2001) *Nat. Struct. Biol.* 8, 756–760.